Desalination and Water Treatment
www.deswater.com
doi: 10.1080/19443994.2014.910839

54 (2015) 3432–3443
June

Taylor & Francis
Taylor & Francis Group

Defluorination from aqueous solution by Ti(IV)-modified granular activated carbon

Dingding Tang, Yuwei Zhao, Yixin Wang, Yijia Yang, Dongyang Li, Tianwei Peng, Xuhui Mao*

School of Resource and Environmental Science, Wuhan University, Wuhan 430072, China, Tel./Fax: +86 27 6877 5799; Email: clab@whu.edu.cn

Received 2 October 2013; Accepted 28 March 2014

ABSTRACT

Fluoride contamination of drinking water and groundwater is a worldwide concerned issue, and technologies are needed for the treatment of aqueous fluoride. In this study, Ti(IV) species-modified granular activated carbon (Ti(IV)-GAC) was prepared and tested for fluoride removal from aqueous solution. Batch experiments were performed to investigate the equilibrium, kinetics, and mechanism of fluoride adsorption onto the prepared Ti(IV)-GAC. The results showed that the spontaneous fluoride adsorption process followed the Langmuir isotherm model and the pseudo-second-order kinetic model. Fluoride adsorption onto the Ti(IV)-GAC was enhanced as the initial fluoride concentration and contact time increased. Alkaline pH and elevated solution temperature did not favor the adsorption of fluoride. Anion exchange between the fluoride ions and the hydroxyl groups of the adsorbents was the major adsorption mechanism. Both batch experiments and flowing column experiments demonstrated that the Ti(IV)-GAC adsorbent can effectively remove the aqueous fluoride with high efficiency, and bring down the fluoride concentration lower than the permissible limit of fluoride in drinking water in China (1.0 mg/L). Experiments also showed that the Ti(IV)-GAC material had favorable regenerability, and can be used as a versatile adsorbent for treating mixed contamination of fluorides and organic pollutants.

Keywords: Defluorination; Granular activated carbon; Adsorption; Ti(IV)

1. Introduction

Fluoride, which mainly comes from the dissolution of minerals in rocks such as fluorospar, cryolite, fluorapatite, etc. is one of the major natural anions present in groundwater. Fluoride can be adsorbed by human body via a series of routes such as drinking water, food, drugs, toothpaste, air, cosmetic, etc. of which drinking water is probably the main route [1]. The effect of fluoride on human teeth and bones depends on its concentration in drinking water. Fluoride is considered beneficial at levels of about 0.7 mg/L but harmful once it exceeds 1.5 mg/L. Excessive fluoride in drinking water may cause dental or skeletal fluorosis, muscle fiber degeneration, low hemoglobin levels, and some other health issues [2,3]. Thus, the permissible limit of fluoride in drinking water suggested by the World Health Organization and being followed in most of the nations is 1.5 mg/L, and in China and Japan, the safe concentration is further limited to

*Corresponding author.

below 1.0 mg/L [4]. High fluoride concentrations in groundwater were reported in many countries [5–8], and it was estimated that more than 260 million people worldwide consume drinking water with a fluoride concentration higher than 1.5 mg/L [1].

So far, a variety of technologies including precipitation-coagulation, membrane-based processes [5,6], and adsorption [1,7,8] have been applied to remove fluoride from water. Usually, the very high concentrations of fluoride in industrial effluents, e.g. from the manufacturing of electrolytic aluminum, semiconductors, glass, chemical fertilizer and steel, etc. [9,10], are treated by the method of precipitation–coagulation, where calcium or magnesium hydroxide slurry was used to reject fluoride as CaF_2 or MgF_2. The effluent concentrations can be brought down to about 10–30 mg/L through this method [11]. The membrane-based process and the adsorption process are suitable for treating the contaminated water with lower fluoride concentrations (10–30 mg/L), so as to bring down fluoride concentration to acceptable limits. In comparison with the membrane-based process, adsorption process retains a major place in defluorination research and practice, due to its greater accessibility and lower cost [1]. At present, researchers have explored many types of adsorbents to remove fluoride from water, such as alumina and aluminum-based adsorbents [12], carbon materials [7], zeolites [8], polymeric material [13], synthetic resins [14], calcium minerals [15], clays and soils [16], layered double hydroxides (LDHs) [17] etc.

In order to improve the performance and decrease the cost of the adsorbents, many attempts have also been made to prepare surface-modified or composite materials for defluoridation. For example, Maliyekkal et al. used a manganese oxide-coated alumina absorbent to bring down the fluoride concentration to the statutory 1.5 mg/L [18]. Tripathy et al. further brought the fluoride concentration down to 0.2 mg/L using manganese dioxide-coated activated alumina adsorbent [19]. Larsen et al. used a composite adsorbent of calcite and brushite to treat the distilled water initially containing 5, 10, and 20 mg/L fluoride, and the concentrations were reduced to 0.06, 0.4, and 5.9 mg/L, respectively [20]. Gupta et al. adopted the waste carbon slurries for defluorination and low fluoride levels (<1.5 mg/L) were achieved [21].

The present study aims to investigate the feasibility of fluoride uptake using modified granular activated carbon (GAC). The reason of selecting GAC as the substrate is its safety and extensive use in drinking water treatment. It is well known that GAC can effectively treat organics, heavy metals, and some inorganic anions in raw water. If a simple modification process enables the GAC capable of uptake of fluoride, little change needs to be made for the existing water treatment facilities and equipment, which are originally designed for GAC absorption technique. Moreover, the versatility and safety of the GAC adsorbents are believed to be retained if a suitable modification is adopted. Therefore, the present study uses the hydrous titanium dioxides derived from titanium sulfate to modify the GAC. The hydrous Ti(IV) species, which are safe for drinking water, can uptake fluoride, while the GAC still possesses the capacity for decontaminating other pollutants like organics. The fundamental aspects of the modified materials (from adsorption isotherms, kinetics to mechanism of fluoride adsorption), and the engineering aspects of the materials (e.g. regenerability, versatility, and flowing adsorption properties), are further studied for a comprehensive evaluation on this new adsorbent.

2. Experimental

2.1. Preparation and characterization of adsorbent

All chemicals used in this study were of ACS grade and obtained from Sinopharm Chemical Reagent, Shanghai, China. The GAC (CAS: 7440-44-0) was first boiled in deionized water for 30 min, then washed with distilled water to remove the impurities, and dried at 80 °C for 24 h. Based on the preliminary experiments, the modified GAC was prepared by mixing 5 g pristine GAC with 100 ml 1 g/L titanium sulfate ($Ti(SO_4)_2$) (CAS: 13693-11-3) in a 200 ml beaker. 1 wt.% sodium hydroxide was used to adjust the solution pH to around 4. The mixture was stirred at room temperature for 4 h and then held for 2 h. After filtration and repeated washing with distilled water, the modified GAC absorbent was finally oven dried at 50 °C for 24 h in the air prior to use and characterization. The loading amount of Ti(IV) species on the pristine GAC was determined using a thermogravimetry analyzer (5 °C/min, from 20 to 800 °C, in the air). An X-ray photoelectron spectrometer (XPS, KRATOS XSAM800 spectrometer) was used to determine the chemical state. The morphologies of the GAC were observed using a scanning electron microscopy (SEM, FEI Sirion field emission).

2.2. Adsorbate and measurement

A stock solution of 100 mg/L fluoride was prepared by dissolving 223.68 mg NaF (CAS: 7681-49-4) in 1 L of deionized water. The working solutions with appropriate concentration were obtained by diluting the stock solution with deionized water. The pH of solution was not adjusted if not otherwise specified. A fluoride ion

selective electrode (model 702, Ruosull, US) was used to determine the fluoride concentrations. The electrode was connected to a pH meter with an expanded millivolt scale (PB-10, sartorius, Germany). The mixture solution including 1 M sodium chloride, 1.2 mM sodium citrate, and 2.5 mM acetic acid was used as the total ionic strength adjustment buffer (TISAB) for determination. The TISAB was added to each standard as well as to the unknown samples (5 vol% with respect to the total volume of solution). According to the calibration curve between the potential values and the fluoride concentrations of standard solutions, the fluoride concentration was calculated.

2.3. Procedure of batch adsorption experiments

Batch experiments were conducted by mixing 1 g as-prepared adsorbents with 50 ml 10 mg/L fluoride solution in a 100 ml polyethene beaker. The solution with initial pH of 6–7 was shaken at 120 rpm at a constant temperature of 25˚C for 2 h, which was more than sufficient for the adsorption equilibrium to be reached. After adsorption, the mixture was centrifuged or filtered by a 0.45 μm PVDF Millipore using syringe filter, and the residual fluoride in the supernatant was determined. 1–2 mL solution was sampled for each determination. If not otherwise specified, all batch experiments followed the above conditions. The equilibrium adsorbed capacity (q_e, mg/g) of fluoride onto modified GAC can be calculated by Eq. (1).

$$q_e = \frac{V(C_0 - C_e)}{m} \tag{1}$$

where V is the solution volume, L; C_0 and C_e are the initial and equilibrium (final) concentration of fluoride, mg/L; and m is the mass of absorbent, g.

Isotherm experiments were conducted at different initial fluoride concentrations (5, 10, 30, 50, 70, and 100 mg/L) at different solution temperatures (25, 35, and 45˚C). Kinetic experiments were conducted at 25˚C using 100 mL fluoride solution (10 mg/L and 5 mg/L initial concentration) and 2 g as-prepared adsorbents. At predetermined times, the residual fluoride concentration (C_t, mg/L) was determined and the amount of fluoride adsorbed onto adsorbents at time t (q_t, mg/g) was calculated by Eq. (2), where C_t is the fluoride concentration at time t in the duration of a batch experiment, mg/L.

$$q_t = \frac{V(C_0 - C_t)}{m} \tag{2}$$

In the tests to evaluate the effect of pH and coexisting anions, the solution pH was adjusted to the desired values using NaOH or HCl solution, and the investigated coexisting anions were 200 mg/L HCO_3^-, CO_3^{2-}, SO_4^{2-}, and Cl^-, which were added in the fluoride-containing solution, respectively. The regenerability of the adsorbent was investigated using 1 wt.% NaOH solution. One gram of saturated absorbent was mixed with 50 ml 1 wt.% NaOH solution, the mixture was then shaken at 120 rpm at ~20˚C for 24 h. After washing with deionized water and dried at 80˚C, the adsorbent was used to adsorb the fluoride again and the adsorption capacity after regeneration was evaluated. The regeneration efficiency (η_{rg}, %) was calculated by Eq. (3), where q_{en} (mg/g) is the adsorption capacity of the regenerated adsorbents after n cycles.

$$\eta_{rg} = \frac{q_{en}}{q_{e(n-1)}} \times 100\% \tag{3}$$

In order to know whether the Ti(IV)-GAC adsorbent possesses the capacity to remove fluoride and organic pollutants simultaneously (i.e. the versatility of the adsorbent), a solution containing 10 mg/L fluoride and 20 mg/L aniline (CAS: 62-53-3) was used for adsorption experiments, and the experiment procedure was as same as the aforementioned batch experiment. Aniline was selected because it is a representative water-soluble organic contaminant that can be adsorbed by GAC. The aqueous aniline concentration was determined using a photo spectrometer at 545 nm wavelength.

2.4. Column experiments

The column breakthrough experiments were carried out in a glass column having dimensions of 19.6 cm height and 2.5 cm diameter. Sixty grams of Ti(IV)-GAC adsorbents were filled in the column. The water-containing fluoride was pumped into the column from the bottom at desired volumetric flow rate using a peristaltic pump (Model DHL-B) supplied by Shanghai Huxi Ltd, China. The process was optimized for the feed fluoride concentration (2–10 mg/L) and flow rate (0.20–0.65 L/h). The effluent samples were collected at different intervals and the residual fluoride concentration was determined using fluoride ion selective electrode.

2.5. Adsorption isotherm

Two commonly used models, the Langmuir isotherm which assumes that adsorption takes place on

homogeneous surfaces and the Freundlich isotherm which assumes that adsorption takes place on heterogeneous surfaces, were selected to simulate the adsorption isotherm. The Langmuir model can be described as Eq. (4), and the dimensionless constant separation factor (R_L) which is used to characterize the adsorption equilibrium can be calculated by Eq. (5), where K_L is the Langmuir equilibrium constant, L/mg; and Q_m is the maximum adsorption capacity, mg/g.

$$q_e = \frac{Q_m K_L C_e}{1 + K_L C_e} \tag{4}$$

$$R_L = \frac{1}{1 + K_L C_0} \tag{5}$$

The Freundlich model can be expressed by Eq. (6), where K_f and n are isotherm constants which indicate the capacity and the intensity of the adsorption, respectively.

$$q_e = K_f \, C_e^{1/n} \tag{6}$$

2.6. Adsorption kinetics

Pseudo-first-order model and pseudo-second-order model are used to investigate the mechanism of adsorption and the transient behavior of fluoride adsorption. The integral form of the pseudo-first-order model is generally described as Eq. (7), where k_s is the adsorption first-order rate constant, min^{-1}; and t is the contact time, min.

$$\log(q_e - q_t) = \log q_e - \frac{k_s}{2.303} t \tag{7}$$

The integral form of the pseudo-second-order model generally described as Eq. (8), where k_2 is the pseudo-second-order rate constant; g/mg min.

$$\frac{t}{q_t} = \frac{t}{q_e} + \frac{1}{k_2 q_e^2} \tag{8}$$

3. Results and discussion

3.1. Characterization of pristine GAC and Ti(IV)-GAC

Fig. 1 presents the SEM images of the pristine GAC and the Ti(IV) species-modified GAC. As shown in Fig. 1, both the pristine GAC and Ti(IV)-GAC present the inhomogeneous porous structure. Little amounts of deposited sediments can be found in the surface pores of the pristine GAC. After modification, an increased amount of deposited sediments can be observed in the pores of GAC. In order to determine the composition of the deposited sediment, XPS analysis was employed to investigate both the pristine GAC and the Ti(IV)-GAC, as depicted in Fig. 2. For the XPS spectrum of the pristine GAC, C *1s* and O *1s* peaks belonging to the activated carbons [22,23], were observed. In case of the modified GAC, a new peak of Ti *2p*, designating the existence of Ti(IV) species, appeared in the spectrum in addition to the C *1s* and O *1s* peaks. The higher resolution spectrum of the Ti *2p* peak (the inset in Fig. 2(b)) further reveals the binding energies of Ti $2p_{1/2}$ (465.1 eV) and Ti $2p_{3/2}$ (458.4 eV) peaks. The two peaks could be assigned to Ti–O bond, suggesting the loaded Ti(IV) species most likely existed in the form of dioxide or hydrated hydroxyl compounds [24]. The XPS results are in accord with a previous report regarding the Ti(IV) species on activated carbon fibers [24]. The characterization of the modified activated carbon samples evidenced the

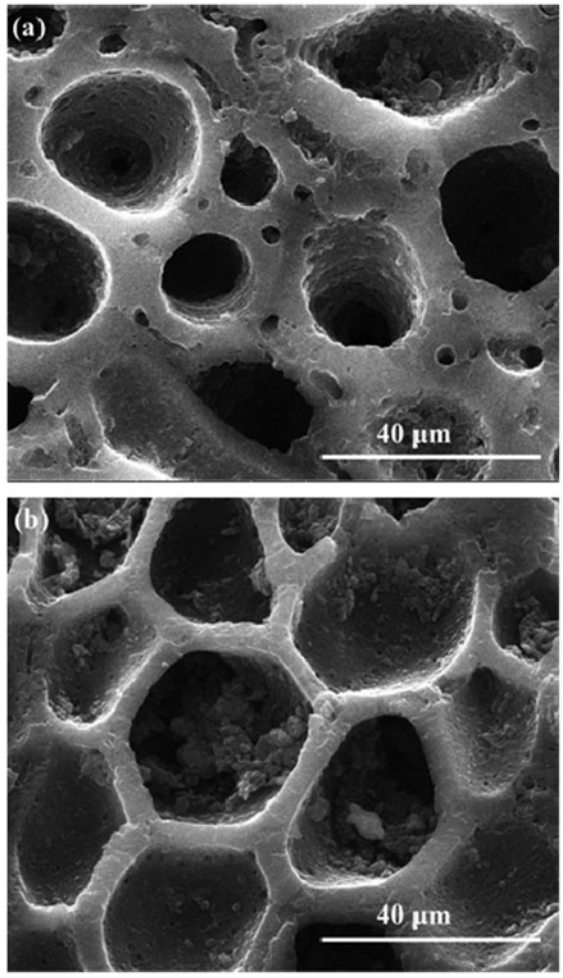

Fig. 1. SEM images of the (a) pristine GAC and (b) Ti(IV) species modified GAC (Ti(IV)-GAC).

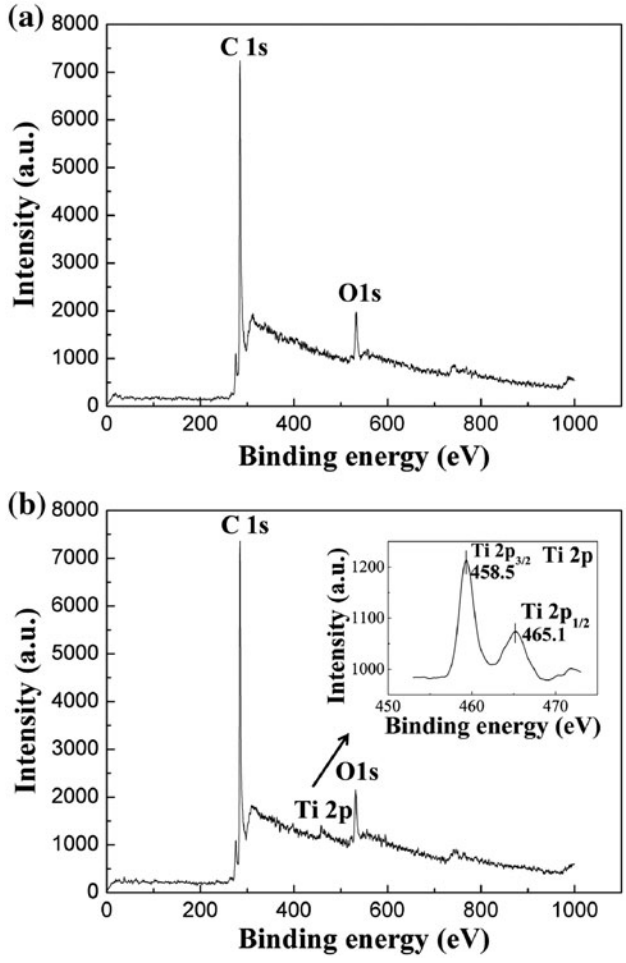

Fig. 2. XPS spectra of the (a) pristine GAC and (b) Ti(IV) species modified GAC (inset is the enlarged Ti 2*p* spectra).

successful loading of the Ti(IV) species on the surface of GAC. The hydrolysis process of $Ti(SO_4)_2$ at elevated pH resulted in the generation of Ti(IV) species with Ti–O bonds.

The loading amount of Ti(IV) species can be measured by a TG analyzer [25]. The results showed that the ratio of residual mass after calcination (i.e. the TG analysis) was 7.23 wt.% for Ti(IV)-GAC, being higher than the 2.24 wt.% residual mass of pristine GAC. The increasing ratio of residual mass (4.99 wt.%) was apparently due to the loaded Ti(IV) species. The loading amount of the Ti(IV) species (TiO_2) onto the GAC was then calculated to be about 49.9 mg/g. Considering that the crystal water is removed at elevated temperatures, we think the real amount of the hydrous Ti (IV) species should be higher than 49.9 mg/g. For example, assuming the stoichiometric composition of the Ti(IV) species before calcination is $Ti(OH)_4$, the loaded Ti(IV)-activated material for defluorination is 72.4 mg/g. That is to say, the average loading amount of hydrated Ti(IV) species should be in the range from 49.9 to 72.4 mg/g.

3.2. Absorption isotherms and kinetics

3.2.1. Adsorption equilibrium isotherm

The adsorption isotherm can be used to describe how the adsorbate interacts with the adsorbent and gives an idea of the adsorption capacity of the adsorbent [26]. The Langmuir isotherm and Freundlich isotherm are valid for monolayer and multilayer adsorptions [27], respectively. Fig. 3(a) shows the comparison of the Langmuir isotherm (Eq. 4) and the Freundlich isotherm (Eq. 6) fittings for Ti(IV)-GAC at three different temperatures (25, 35, and 45˚C). Isotherm parameters obtained by the fitting are listed in Table 1. From Table 1, the correlation coefficients (R^2) suggest that the Langmuir isotherm shows a better fit to adsorption data than the Freundlich isotherm at all temperatures, indicating that the adsorption of fluoride on Ti(IV)-GAC is a monolayer adsorption process [27]. When C_e is around 47.5 mg/L, the maximum adsorption capacity (Q_m) increases from 2.62 to 2.87 mg/g with the decrease in temperature from 45 to 25 ˚C. The dimensionless constant separation factor R_L, which expresses the essential features of the Langmuir isotherm [28], is used to predict if the adsorption process is "favorable" or "unfavorable." The R_L calculated by Eq. (5) is shown in Fig. 3(b). Apparently, R_L is always in the range between 0 and 1, which implies that the fluoride adsorption onto Ti(IV)-GAC is "favorable" for all cases [29]. Moreover, the value of R_L decreases as the initial fluoride concentration increases and the solution temperature decreases, implying that higher fluoride concentrations and lower temperatures are more conductive to the fluoride adsorption onto Ti(IV)-GAC.

3.2.2. Adsorption kinetics

Fig. 4 presents the kinetics of fluoride adsorption onto Ti(IV)-GAC. As can be observed, the amount of adsorbed fluoride (q_t) increased with time and eventually reached equilibrium (q_e) within 40 min. The first stage of adsorption was signified by a steep slope, reflecting the rapid adsorption rate during the first 10 min of contact. In this stage, around 75% of the adsorption capacity was realized. The rapid adsorption rate is mainly due to instantaneous monolayer adsorption of fluoride at the surface of Ti(IV)-GAC. The second stage which took place between 10 and 40 min, characterized a gentle slope and a gradually

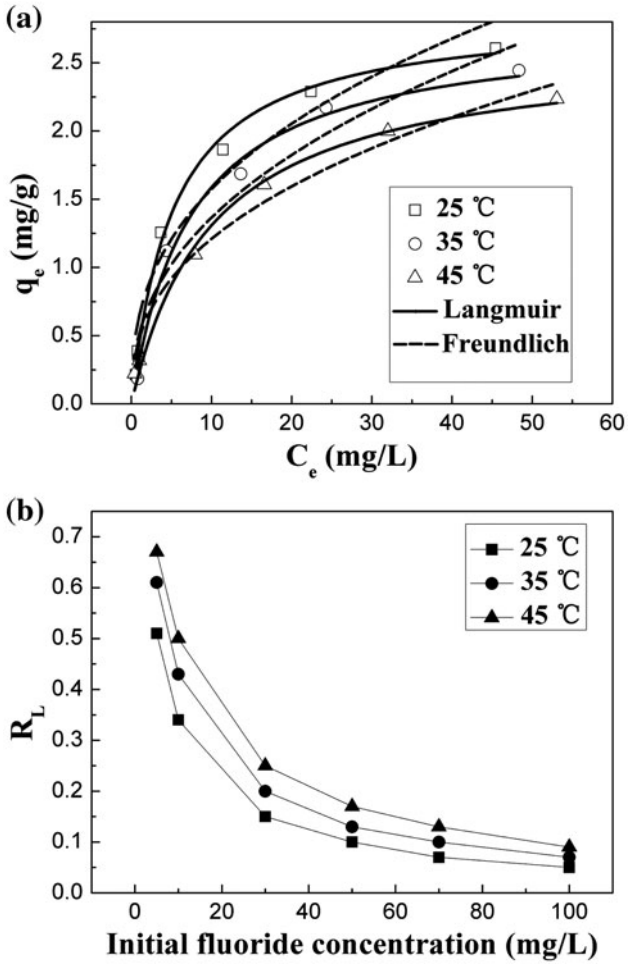

Fig. 3. (a) Adsorption isotherms of fluoride adsorption onto Ti(IV)-GAC (at 25, 35 and 45 ℃), and the fitting curves by the Langmuir model and Freundlich model. (b) Changes of dimensionless constant separation factor R_L as a function of initial fluoride concentrations (5, 10, 30, 50, 70 and 100 mg/L).

Table 1
Parameters of the data fitting using the Langmuir and Freundlich isotherm models

Model	Parameter	Temperature 25℃	35℃	45℃
Langmuir isotherm	R^2	0.9934	0.9886	0.9812
	Q_m (mg/g)	2.87	2.77	2.62
	K_L (L/mg)	0.19	0.13	0.10
Freundlich isotherm	R^2	0.9307	0.9364	0.9442

decreasing adsorption rate. The reduced adsorption rate is probably attributed to the rearrangement of fluoride adsorbed on the Ti(IV)-GAC surface and a more thorough utilization of adsorption sites on the Ti

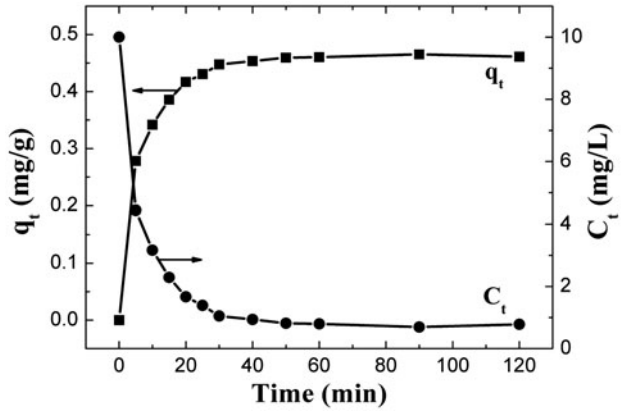

Fig. 4. Kinetics of fluoride adsorption onto Ti(IV)-GAC adsorbents and the residual fluoride concentration (at 25℃).

(IV)-GAC [30,31]. After 40 min of contact time, the adsorption of fluoride basically reached equilibrium. Correspondingly, the residual concentration of fluoride in solution decreased as the fluoride adsorption reaction progressed. As can be observed, after 40 min of adsorption, the residual concentration of fluoride decreased from 10 mg/L to 0.93 mg/L, which is lower than the permissible limit of fluoride in drinking water (1 mg/L in China). The final residual fluoride concentration was 0.70 mg/L after 120 min of contact. Under the same experimental conditions, the residual fluoride concentration achieved by the pristine GAC was 9.97 mg/L. The result indicates that the Ti(IV) modified GAC is much more efficient than the pristine GAC for defluorination process.

The applicability of the pseudo-first-order and pseudo-second-order models [32] was tested for the adsorption of fluoride onto Ti(IV)-GAC. Fig. 5 shows the fitting results at the initial fluoride concentration of 10 mg/L. As can be seen, the linear correlation coefficients for the pseudo-second-order model are greater than these of the pseudo-first-order model. Furthermore, the equilibrium adsorption capacities (q_e) predicted by the pseudo-first-order kinetic model (Eq. 7) apparently deviated from the experimental values, while the q_e predicted by the pseudo-second-order model (Eq. (8)) was very close to the experimental values.

The kinetic modeling can be further validated by the half-life time of fluoride, since the modeling may be affected by the initial concentration of the contaminant [33]. For the pseudo-first-order kinetic reaction, the sorption processes occur at a rate proportional either to fluoride concentration, or to the number of vacant sorption sites; therefore, the half-life time of adsorbate is constant whatever the initial concentration. For the pseudo-second-order kinetic reaction, it is

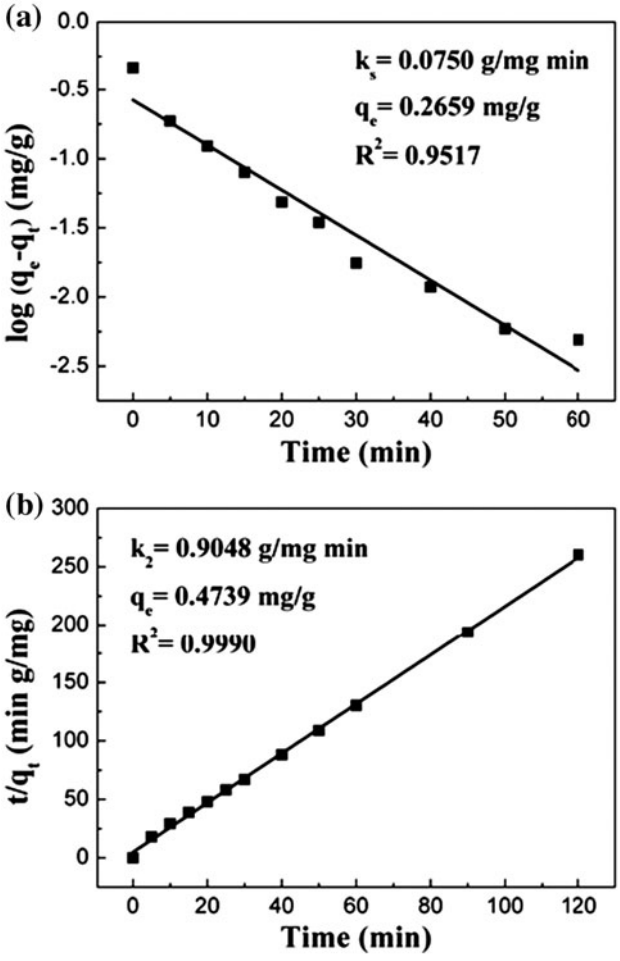

Fig. 5. (a) Pseudo-first-order kinetic model and (b) pseudo-second-order kinetic model for the adsorption of 10 mg/L fluoride at 25°C.

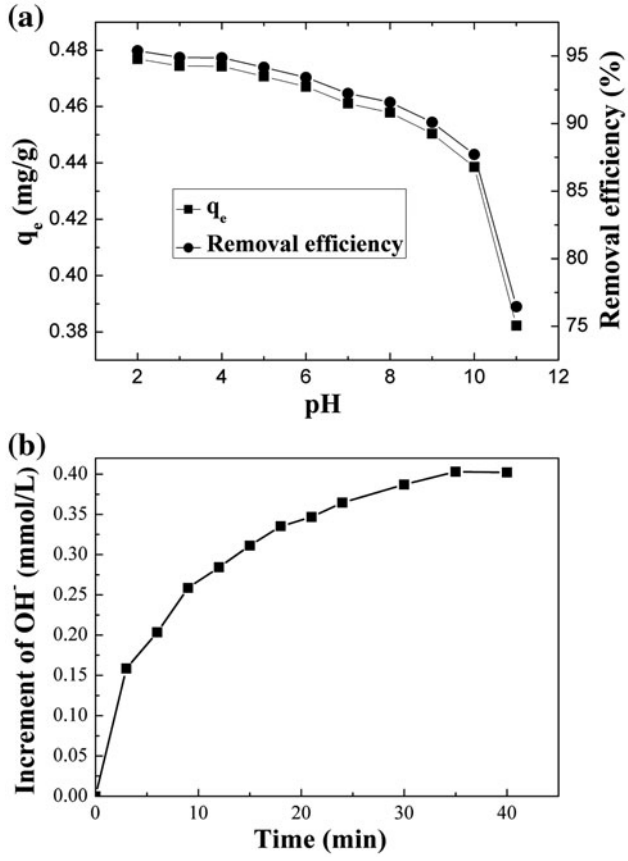

Fig. 6. (a) Effect of pH on the fluoride adsorption onto Ti (IV)-GAC and (b) the increment of OH^- with contact time.

thought to derive from sorption processes in which the rate-controlling step is an "exchange reaction," and the half-life time varies with the initial concentration [34]. Therefore, extra kinetic experiments were carried out at an initial fluoride concentration of 5 mg/L. The results showed that the half-life time of fluoride adsorption decreased from 3.29 to 2.33 min when the initial fluoride concentration was elevated from 5 to 10 mg/L. The changed half-life time confirms the better applicability of the pseudo-second-order model for describing the adsorption of fluoride onto Ti(IV)-GAC.

3.3. Effect of pH and coexisting anions

3.3.1. Effect of pH

The effect of pH on fluoride adsorption onto Ti(IV)-GAC was studied in the range of 2–11 (Fig. 6(a)). As can be seen, the amount of fluoride adsorbed by Ti(IV)-GAC decreased from 0.477 mg/g to 0.382 mg/g due to the variation of pH from 2 to 11. Correspondingly, the removal efficiency of fluoride decreased from 95.38 to 76.45%. The results show that high pH inhibited the fluoride adsorption onto the Ti(IV)-GAC absorbents.

XPS analysis results in Section 3.1 have revealed that the loaded Ti(IV) species existed in the form of dioxide or hydrated hydroxyl compounds, which derived from the hydrolytic process of $Ti(SO_4)_2$ at elevated pHs. It was reported that the anion exchange between fluoride ions and hydroxyl groups of adsorbent could be the mechanism of fluoride uptaking by some minerals [35]. Fluoride ions bonded with the adsorbent, and hydroxyl ions released from adsorbent into the solution to maintain the charge balance. Therefore, we investigated the change of the solution pH during the adsorption process, and the concentration of hydroxyl ions was calculated and depicted as a function of contact time. As can be observed, the amount of hydroxyl ions gradually increased as the

adsorption process progressed. The results suggest that the following defluorination process may proceed on the surface of Ti(IV)-GAC absorbents:

$$(TiO_2)_nTi(OH)_4 + mF^- = (TiO_2)_nTi(OH)_{4-m}F_m + mOH^-$$

$$n \le 0, 0 \le m \le 4 \quad (9)$$

$(TiO_2)_nTi(OH)_4$ is the hydrolyzate of $Ti(SO_4)_2$ in the form of partial ($n > 0$) or absolute ($n = 0$) hydrate. The hydroxyl groups of $(TiO_2)_nTi(OH)_4$ are partially ($m < 4$) or completely ($m = 4$) replaced by fluoride and then released in the solution. This anion-exchange mechanism further illustrates that the reaction process can be retarded under an alkaline condition because it became harder for the reaction to move to the right direction in the presence of more hydroxyl ions. To ensure the function of the adsorbents, the solution pH should be controlled within an appropriate range away from alkaline condition (pH < 9).

3.3.2. Effect of coexisting anions

The effect of coexisting anions on fluoride adsorption onto Ti(IV)-GAC was determined by adding four types of anions (CO_3^{2-}, HCO_3^-, SO_4^{2-}, and Cl^-) into the fluoride working solution, respectively. These anions are common for groundwater (e.g. $HCO_3^-$and HCO_3^- in karstic aquifer) or surface water [36,37]. The removal efficiencies of fluoride in the presence of coexisting anions are shown in Fig. 7. We can observe that all the coexisting anions exhibited negative effect on the fluoride adsorption. Specifically, the removal efficiencies decrease from 92.2% (absence of coexisting anion) to 91.54, 90.51, 88.39, and 87.60% in the presence of 200 mg/L Cl^-, SO_4^{2-}, HCO_3^-, and CO_3^{2-}, respectively. The anions reduced the fluoride adsorption in the following order, $CO_3^{2-} > HCO_3^- > SO_4^{2-} > Cl^-$. The decrease of the removal efficiency was attributed to the competitive adsorption of coexisting anions. Moreover, the presence of HCO_3^- and CO_3^{2-} increased the solution pH, which further account for the stronger inhibition on the fluoride adsorption. It should be pointed out that all the negative effects of the four types of coexisting anions were inconspicuous. The coexisting anions should not be a major concerned issue for the defluorination process.

3.4. Regenerability and versatility of the Ti(IV)-GAC

To determine the regenerability of the prepared Ti (IV)-GAC, 1 wt% NaOH was used to treat the saturated Ti(IV)-GAC adsorbent and its regeneration was conducted for consecutive times. The results are depicted in Fig. 8. It can be observed that the fluoride adsorption capacities decreased with the regeneration cycles. After successive regeneration cycles, the removal efficiency, respectively, decreased to 90.92, 88.56, and 86.90%, and the regeneration efficiencies (calculated by Eq. (3)) were 98.59, 97.40, and 98.13%, respectively. The recovered removal efficiency after three regeneration cycles still remained 94.23% of the initial adsorption capacity.

A rough comparison can be made between the prepared Ti(IV)-GAC and some previously reported defluorination materials under the condition of same initial fluoride concentration. Table 2 shows the

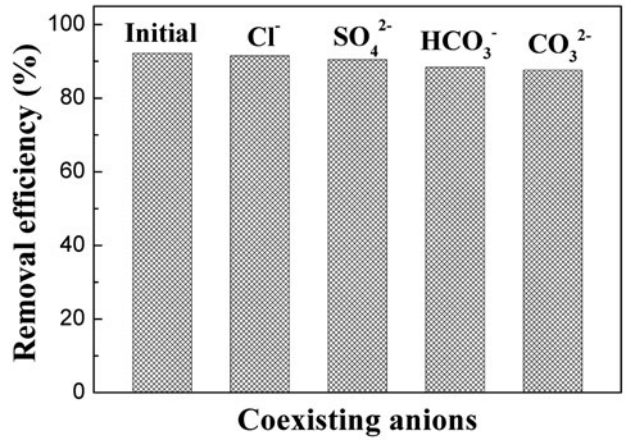

Fig. 7. Effect of the coexisting anions on the fluoride adsorption onto Ti(IV)-GAC.

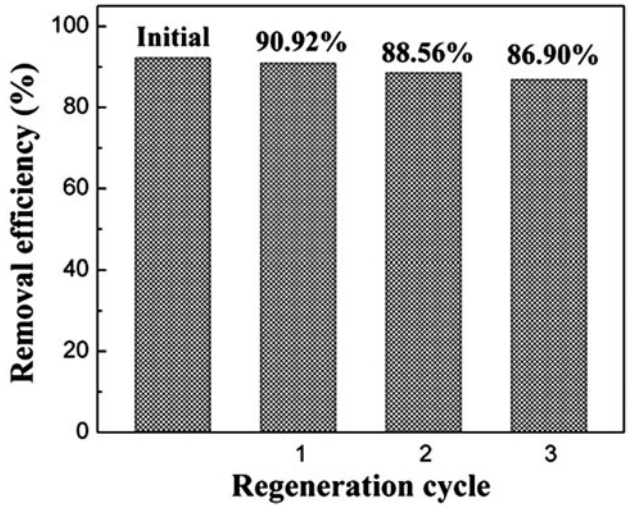

Fig. 8. Fluoride removal efficiency obtained by the fresh prepared and regenerated Ti(IV)-GAC adsorbents.

Table 2
Comparison of the prepared Ti(IV)-GAC with other reported defluorination materials

Adsorbent	pH	Dosage (g/L)	q_e (mg/g)	C_0 (mg/L)	C_e (mg/L)	Removal efficiency (%)
Hydrous manganese oxide-coated alumina [38]	5.2	5	1.8	10.2	1.2	88.2
Synthetic siderite [39]	6.9	20	0.419	10	1.62	83.8
Schwertmannite [40]	3.8	1	9	10	~1	79
Magnesium incorporated bentonite clay [41]	6–7	0.5	6.2	10	6.9	31
Manganese dioxide-coated activated alumina [19]	7	8	1.23	10	0.2	98
Ti(IV)-GAC (this study)	7	20	0.46[a]	10	0.78	92.2

[a]Calculated in terms of the adsorbent mass including the GAC and the loaded Ti(IV) species.

detailed information regarding the solution pH, dosage, $q_{e,}$ and the final fluoride concentration (C_e). It can be observed that, at the dosage of 20 g/L, the Ti(IV)-GAC adsorbent can decrease the fluoride concentration from 10 to 0.78 mg/L, and achieve 92.2% fluoride removal efficiency. The final fluoride concentration is lower than the permissible drinking water standard (1 mg/L) and removal efficiency is only inferior to the manganese dioxide-coated activated alumina. On the other hand, at the dosage of 20 g/L, the equilibrium adsorption capacity (q_e) seems not competitive. Among the listed materials, the q_e of Ti(IV)-GAC is only higher than that of the synthetic siderite. The effective component of Ti(IV)-GAC for defluorination is hydrous Ti(IV) species, and its average loaded amount is less than 72.4 mg/g, as indicated in Section 3.1. Therefore, we did not observe a high q_e value for the Ti(IV)-GAC adsorbent, even though the hydrous Ti(IV) species could be an excel defluorination material.

Comparing with the "bulk" defluorination materials like alumina and mineral particles, the Ti(IV)-GAC adsorbent shows a lesser q_e value, however, the properties of the carbon material, e.g. porosity and affinity to organics, is still retained. A separated experiment was carried out in the laboratory to test the versatility of the Ti(IV)-GAC adsorbent, where the adsorption performance of the pristine GAC and Ti(IV)-GAC adsorbents were investigated in the presence of fluoride and aniline at pH 6. The results showed that, with the dosage of 20 g/L, the Ti(IV)-GAC adsorbent can remove fluoride by 90.7% and aniline by 95.0%, respectively. In contrast, at the same dosage of 20 g/L, the pristine GAC removed only 2.2% of the aqueous fluoride, although the aniline removal efficiency was 98.5%. The observation reveals that the modification process enables the GAC particles capable of uptaking fluorides and organics simultaneously. The Ti(IV)-GAC can actually work as a versatile adsorbent for treating the raw water with a mixed contamination of fluoride and organics.

3.5. Column experiments

3.5.1. Effect of flow rate of fluoride solution

The effect of flow rate of the feed fluoride solution was studied at a fixed fluoride concentration of

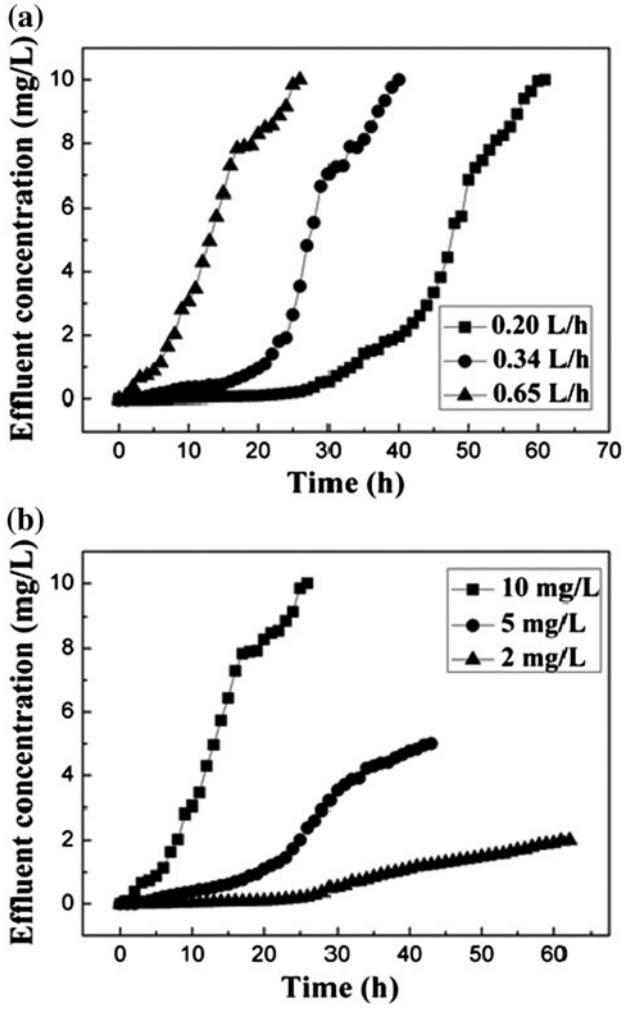

Fig. 9. Effect of the (a) flow rate and (b) initial concentration of the fluoride solution on the breakthrough curves.

Table 3
Detailed parameters of the column experiments

C_0 (mg/L)	Flow rate (L/h)	Breakthrough capacity (L/g)		Adsorption capacity (mg/g)	
		BP = C_0 (BP-a)	BP = 1 mg/L (BP-b)	BP = C_0 (BP-a)	BP = 1 mg/L (BP-b)
10	0.20	0.203	0.113	1.54	1.11
10	0.34	0.227	0.110	1.52	1.08
10	0.65	0.271	0.054	1.33	0.51
5	0.65	0.466	0.217	1.40	1.00
2	0.65	0.672	0.412	0.853	0.76

10 mg/L. The breakthrough curves at three different flow rates (0.20, 0.34, and 0.65 L/h) are shown in Fig. 9(a), and the corresponding parameters are shown in Table 3. It is noted that two kinds of breakthrough points (BP-a and BP-b) are defined in Table 3: the effluent fluoride concentration is as high as the influent fluoride concentration (BP-a), or effluent fluoride concentration exceeds 1 mg/L (BP-b). As can be observed from Fig. 9(a) and Table 3, increased flow rate causes sharper breakthrough curves and lesser breakthrough times, but its effect on breakthrough capacity is dependent on the types of breakthrough point (BP-a and BP-b). In case of the BP-a, the breakthrough capacity slightly increased from 0.203 to 0.271 L/g as the flow rates changed from 0.20 to 0.65 L/h. In contrast, for the BP-b, we can observe a considerable decrease of breakthrough capacity at 0.65 L/h with respect to the 0.20 and 0.34 L/h flow rates. The dissimilar trends of breakthrough capacity suggest that overquick flow may cause very low breakthrough capacity if the breakthrough point is set at a low effluent concentration like 1 mg/L. This observation is associated with the less hydraulic retention time (HRT) of the liquid at higher flow rates. Less HRT results in an inadequate interaction between the adsorbent and adsorbate, especially at a very high flow rate. Likewise, the adsorption capacity at 0.65 L/h shows a sudden decrease for BP-b, while the other adsorption capacity values are all higher than 1 mg/L. Furthermore, it can observed that the adsorption capacity of the adsorbents basically decreases along with the increasing flow rates, indicating that lower flow rates do facilitate the utilization of the adsorbents.

3.5.2. Effect of initial concentration of fluoride solution

Fluoride uptake within the Ti(IV)-GAC-filled column was investigated with different fluoride concentrations, viz. 2, 5, and 10 mg/L at a fixed flow rate of the fluoride solution (0.65 L/h). The typical breakthrough curves are shown in Fig. 9(b). Sharper breakthrough curve was obtained at higher feed fluoride concentrations. Based on the breakthrough curves, the calculated parameters are also shown in Table 3. In case of the BP-a, the breakthrough time increases from 25 to 62 h as the initial concentration decreases from 10 to 2 mg/L. Accordingly, the breakthrough capacity increases from 0.271, 0.466 to 0.672 L/g. As for the adsorption capacity, it is interesting to note that it increases from 1.33 to 1.40 mg/g, are followed by a decrease down to 0.853 mg/g (see the BP-a). This observation suggests that the highest adsorption efficiency of Ti(IV)-GAC adsorbents occurred at 5 mg/L initial fluoride concentration. As the breakthrough point is set at 1 mg/L (see the BP-b), the breakthrough capacity is found to be 0.412, 0.217, and 0.054 L/g at initial concentrations of 2, 5, and 10 mg/L, respectively. The highest adsorption capacity still occurred at the initial concentration of 5 mg/L, being 1 mg/g.

4. Conclusion

In the present study, a new adsorbent, Ti(IV) species-modified GAC (Ti(IV)-GAC) was prepared and its fluoride adsorption behaviors were investigated. SEM, XPS, and TG characterization showed that Ti(IV) species, were successfully loaded onto the GAC. The Ti (IV)-GAC featured a fast adsorption and a high removal efficiency of 92.2% at an initial fluoride concentration of 10 mg/L. The residual fluoride concentration could be decreased to 0.7 mg/L, which met the requirement of the safe drinking water standard in China (<1.0 mg/L). The Langmuir isotherm model gave better fittings with the experimental data than the Freundlich model, indicating that the adsorption of fluoride onto Ti(IV)-GAC is a monolayer adsorption process. The adsorption kinetic data were better described by the pseudo-second-order model than by the pseudo-first-order model. The equilibrium adsorption capacity of Ti(IV)-GAC increased with initial fluoride concentration and contact time, but decreased with temperature and solution pH. The major adsorption mechanism of fluoride is anion

exchange between fluorides and hydroxyls. Tests also demonstrated that the Ti(IV)-GAC absorbent showed well regenerability in aqueous solution, and was able to treat fluoride and aniline simultaneously. The flowing column experiments revealed that the breakthrough capacity (L/g) and adsorption capacity (mg/L) of Ti(IV)-GAC absorbent was strongly dependent on the flow rate and inlet fluoride concentration, and the operation parameters of column can be optimized for effective defluorination. This study demonstrates that a simple chemical modification of the GAC could be an optional route to prepare a versatile adsorption material, which can be engineered to treat mixed contamination of fluoride and organic micropollution.

Acknowledgments

The project described was supported by the Nature Science Foundation of China (NSFC Grant No. 51108353 and 51278386) and the scientific research training project of geographical science major (No. J1103409).

Symbols

C_0 — initial fluoride concentration (mg/L)
C_e — equilibrium (final) fluoride concentration (mg/L)
C_t — fluoride concentration at contact time t (mg/L)
k_s — pseudo-first-order rate constant (min^{-1})
k_2 — pseudo-second-order rate constant (g/mg min)
K_L — Langmuir equilibrium constant (L/mg)
K_f — Freundlich constant indicative of the relative sorption capacity of the sorbent (mg/g)
M — mass of absorbent (g)
N — Freundlich constant indicative of the intensity of sorption
q_e — equilibrium adsorption capacity (mg/g)
q_{en} — adsorption capacity of the regenerated adsorbents after n cycles (mg/g)
q_t — amount of the fluoride adsorbed onto adsorbents at time t (mg/g)
Q_m — maximum adsorption capacity (mg/g)
R_L — dimensionless constant separation factor for the Langmuir isotherm model (mg/g)
T — time t
V — solution volume (L)
η_{rg} — regeneration efficiency of adsorbent (%)

References

[1] M. Mohapatra, S. Anand, B. Mishra, D.E. Giles, P. Singh, Review of fluoride removal from drinking water, J. Environ. Manage. 91 (2009) 67–77.
[2] M. Ansari, M. Kazemipour, M. Dehghani, M. Kazemipour, The defluoridation of drinking water using multi-walled carbon nanotubes, J. Fluorine Chem. 132 (2011) 516–520.
[3] S. Jagtap, M.K. Yenkie, N. Labhsetwar, S. Rayalu, Fluoride in drinking water and defluoridation of water, Chem. Rev. 112 (2012) 2454–2466.
[4] G. Zhang, Z. He, W. Xu, A low-cost and high efficient zirconium-modified-Na-attapulgite adsorbent for fluoride removal from aqueous solutions, Chem. Eng. J. 183 (2012) 315–324.
[5] M. Arora, R. Maheshwari, S. Jain, A. Gupta, Use of membrane technology for potable water production, Desalination 170 (2004) 105–112.
[6] A. Lhassani, M. Rumeau, D. Benjelloun, M. Pontie, Selective demineralization of water by nanofiltration application to the defluorination of brackish water, Water Res. 35 (2001) 3260–3264.
[7] S. Márquez-Mendoza, M. Jiménez-Reyes, M. Solache-Ríos, E. Gutiérrez-Segura, Fluoride removal from aqueous solutions by a carbonaceous material from pyrolysis of sewage sludge, Water Air Soil Poll. 223 (2012) 1959–1971.
[8] M.S. Onyango, Y. Kojima, O. Aoyi, E.C. Bernardo, H. Matsuda, Adsorption equilibrium modeling and solution chemistry dependence of fluoride removal from water by trivalent-cation-exchanged zeolite F-9, J. Colloid Interface Sci. 279 (2004) 341–350.
[9] P. Ndiaye, P. Moulin, L. Dominguez, J. Millet, F. Charbit, Removal of fluoride from electronic industrial effluentby RO membrane separation, Desalination 173 (2005) 25–32.
[10] F. Shen, X. Chen, P. Gao, G. Chen, Electrochemical removal of fluoride ions from industrial wastewater, Chem. Eng. Sci. 58 (2003) 987–993.
[11] M. Chang, J. Liu, Precipitation removal of fluoride from semiconductor wastewater, J. Environ. Eng. 133 (2007) 419–425.
[12] V.S. Chauhan, P.K. Dwivedi, L. Iyengar, Investigations on activated alumina based domestic defluoridation units, Hazard. Mater. 139 (2007) 103–107.
[13] M. Karthikeyan, K. Kumar, K. Elango, Batch sorption studies on the removal of fluoride ions from water using eco-friendly conducting polymer/bio-polymer composites, Desalination 267 (2011) 49–56.
[14] S. Meenakshi, N. Viswanathan, Identification of selective ion-exchange resin for fluoride sorption, J. Colloid Interface Sci. 308 (2007) 438–450.
[15] M. Yang, T. Hashimoto, N. Hoshi, H. Myoga, Fluoride removal in a fixed bed packed with granular calcite, Water Res. 33 (1999) 3395–3402.
[16] S. Meenakshi, C.S. Sundaram, R. Sukumar, Enhanced fluoride sorption by mechanochemically activated kaolinites, J. Hazard. Mater. 153 (2008) 164–172.
[17] L. Lv, J. He, M. Wei, D. Evans, Z. Zhou, Treatment of high fluoride concentration water by MgAl-CO_3 layered double hydroxides: Kinetic and equilibrium studies, Water Res. 41 (2007) 1534–1542.
[18] S.M. Maliyekkal, A.K. Sharma, L. Philip, Manganese-oxide-coated alumina: a promising sorbent for defluoridation of water, Water Res. 40 (2006) 3497–3506.
[19] S.S. Tripathy, A.M. Raichur, Abatement of fluoride from water using manganese dioxide-coated activated alumina, J. Hazard. Mater. 153 (2008) 1043–1051.
[20] M. Larsen, E. Pearce, Defluoridation of drinking water by boiling with brushite and calcite, Caries Res. 36 (2002) 341–346.

[21] V.K. Gupta, I. Ali, V.K. Saini, Defluoridation of wastewaters using waste carbon slurry, Water Res. 41 (2007) 3307–3316.
[22] A.P. Terzyk, The influence of activated carbon surface chemical composition on the adsorption of acetaminophen (paracetamol) *in vitro*, Colloid Surf. A-Physicochem. Eng. Asp. 177 (2001) 23–45.
[23] R. Jansen, H. Van Bekkum, XPS of nitrogen-containing functional groups on activated carbon, Carbon 33 (1995) 1021–1027.
[24] P. Fu, Y. Luan, X. Dai, Preparation of activated carbon fibers supported TiO_2 photocatalyst and evaluation of its photocatalytic reactivity, J. Mol. Catal. A: Chem. 221 (2004) 81–88.
[25] L.C. Oliveira, R.V. Rios, J.D. Fabris, V. Garg, K. Sapag, R.M. Lago, Activated carbon/iron oxide magnetic composites for the adsorption of contaminants in water, Carbon 40 (2002) 2177–2183.
[26] S. Dawood, T.K. Sen, Removal of anionic dye Congo red from aqueous solution by raw pine and acid-treated pine cone powder as adsorbent: Equilibrium, thermodynamic, kinetics, mechanism and process design, Water Res. 46 (2012) 1933–1946.
[27] L. Rome, G.M. Gadd, Copper adsorption by *Rhizopus arrhizus*, Cladosporium resinae and Penicillium italicum, Appl. Microbiol. Biotechnol. 26 (1987) 84–90.
[28] A. Bhatnagar, A. Jain, A comparative adsorption study with different industrial wastes as adsorbents for the removal of cationic dyes from water, J. Colloid Interface Sci. 281 (2005) 49–55.
[29] D. Karadag, Y. Koc, M. Turan, B. Armagan, Removal of ammonium ion from aqueous solution using natural Turkish clinoptilolite, J. Hazard. Mater. 136 (2006) 604–609.
[30] S. Baidas, B.Y. Gao, X.G. Meng, Perchlorate removal by quaternary amine modified reed, J. Hazard. Mater. 189 (2011) 54–61.
[31] X. Xu, Y. Gao, B.Y. Gao, X. Tan, Y.Q. Zhao, Q.Y. Yue, Y. Wang, Characteristics of diethylenetriamine-cross-linked cotton stalk/wheat stalk and their biosorption capacities for phosphate, J. Hazard. Mater. 192 (2011) 1690–1696.
[32] Y.-S. Ho, G. McKay, Pseudo-second order model for sorption processes, Process Biochem. 34 (1999) 451–465.
[33] E. López, B. Soto, M. Arias, A. Núñez, D. Rubinos, M. Barral, Adsorbent properties of red mud and its use for wastewater treatment, Water Res. 32 (1998) 1314–1322.
[34] Z. Reddad, C. Gerente, Y. Andres, P. Le Cloirec, Adsorption of several metal ions onto a low-cost biosorbent: Kinetic and equilibrium studies, Environ. Sci. Technol. 36 (2002) 2067–2073.
[35] J. Zhang, S. Xie, Y.-S. Ho, Removal of fluoride ions from aqueous solution using modified attapulgite as adsorbent, J. Hazard. Mater. 165 (2009) 218–222.
[36] W. Stumm, J.J. Morgan, Aquatic Chemistry. John Wiley & Sons, New York, NY, 1996.
[37] D. Langmuir, Aqueous Environmental Geochemistry. Prentice Hall, New York, NY, 1997.
[38] S.-X. Teng, S.-G. Wang, W.-X. Gong, X.-W. Liu, B.-Y. Gao, Removal of fluoride by hydrous manganese oxide-coated alumina: performance and mechanism, J. Hazard. Mater. 168 (2009) 1004–1011.
[39] Q. Liu, H. Guo, Y. Shan, Adsorption of fluoride on synthetic siderite from aqueous solution, J. Fluorine Chem. 131 (2010) 635–641.
[40] A. Eskandarpour, M.S. Onyango, A. Ochieng, S. Asai, Removal of fluoride ions from aqueous solution at low pH using schwertmannite, J. Hazard. Mater. 152 (2008) 571–579.
[41] D. Thakre, S. Rayalu, R. Kawade, S. Meshram, J. Subrt, N. Labhsetwar, Magnesium incorporated bentonite clay for defluoridation of drinking water, J. Hazard. Mater. 180 (2010) 122–130.